Mapping of the Cleavage-Associated Bleomycin Binding Site on DNA with a New Method Based on Site-Specific Blockage of the Minor Groove with N^2-Isobutyrylguanine†

Dongchul Suh and Lawrence F. Povirk*

Department of Pharmacology and Toxicology, Medical College of Virginia, Virginia Commonwealth University, Richmond, Virginia 23298

Received December 3, 1996; Revised Manuscript Received January 28, 1997⊗

ABSTRACT: Although the binding of various forms of bleomycin to DNA has been studied extensively, the transient nature of the activated bleomycin species which ultimately attacks DNA has largely precluded direct examination of its physical interactions with DNA. In an attempt to map the minimum binding site required for this species to effect DNA cleavage, several oligonucleotide duplexes were synthesized, each of which contained a single N^2-isobutyrylguanine moiety at a specific position in the sequence. These duplexes were end-labeled, and sequence-specific bleomycin-induced cleavage was assessed in each strand of each duplex. Isobutyrylguanine substitution immediately 5′ to a primary bleomycin target site suppressed bleomycin-induced cleavage by more than 10-fold. Substitution two bases 5′ to a target site suppressed cleavage by about 4-fold, and substitution directly opposite the target site suppressed cleavage by 7-fold. Substitution immediately 3′ to the target site, or at other more distant positions 3′ or 5′, had little or no effect. In cases where cleavage at a primary site was strongly suppressed, cleavage at the corresponding secondary site (the putative site of the second break in a bleomycin-induced double-strand break) was also inhibited, even when the secondary site was several bases away from the isobutyrylguanine substitution. The results suggest that the binding site required for bleomycin-induced DNA cleavage spans a region of approximately 2 or 3 bp in the minor groove, including the base associated with the sugar attacked and one or two bases to its 5′ side. Computer-based molecular modeling indicated that these results are consistent with the predictions of recently proposed models in which the bithiazole is intercalated immediately 3′ to the cleavage site, and the iron coordination site binds in the minor groove immediately 5′ to the cleavage site. Both the empirical data and the modeling studies suggest that N^2-isobutyrylguanine substitution effectively blocks the minor groove, but without significantly disturbing DNA secondary structure. Thus, it is proposed that site-specific incorporation of N^2-isobutyrylguanine may provide a general method for mapping binding sites of minor groove-binding ligands on DNA.

The activation of bleomycin proceeds by a multistep process in which the last detectable species formed prior to DNA damage is an Fe(III) complex, believed to have the structure bleomycin·Fe(III)·OOH^-, or bleomycin ferric peroxide (Burger et al., 1981; Kuramochi et al., 1981). Though this species has been termed "activated bleomycin", it is probably only a precursor to yet another species, perhaps a high-valence Fe(IV) or Fe(V) complex, which ultimately abstracts hydrogen from the C-4′ position of deoxyribose in DNA (Stubbe & Kozarich, 1987; Hecht, 1986). The transient nature of both activated bleomycin and its presumed high-valence product largely precludes most types of direct physical−chemical studies of their interactions with DNA. Therefore, studies of bleomycin binding to DNA have commonly been performed with various more stable analogues, such as metal-free bleomycin or its chelate complexes with Cu(II), Zn(II), Co(III), and Fe(III) (Nightingale & Fox, 1994; Povirk et al., 1981; Manderville et al., 1994; Wu et al., 1994). While these studies have given useful information on the nature of bleomycin−DNA interactions, it is virtually impossible to predict whether specific features of DNA binding by any of these analogues will also apply to the transient species that actually attacks DNA. The extent of this limitation is demonstrated by the two very different models of bleomycin−DNA binding derived from NMR studies of Zn(II)·bleomycin (Manderville et al., 1994) and of Co(III)·bleomycin (Wu et al., 1994) bound to oligonucleotide duplexes. Even different forms of Co(III)·bleomycin appear to have markedly different binding geometries (Mao et al., 1996).

One fundamental question that remains unresolved is the extent of the bleomycin binding site on double-stranded DNA. Studies of hydroxyl radical protection and photoactivated DNA cleavage by Co(III)·bleomycin have led to estimates of between two and four bp (Nightingale & Fox, 1994; Kuwahara & Sugiura, 1988); however, in addition to the uncertainty in size, the position of the binding site with respect to the cleavage site is unclear, and again, there is no assurance that the results obtained with the Co(III) form can be extrapolated to the iron−bleomycin species that attack DNA.

The present study describes the use of oligonucleotides incorporating a site-specific minor groove-blocking base

† This work was supported by Grant CA40615 from the National Cancer Institute, U.S. Department of Health and Human Services. D.S. was supported in part by Training Grant CA09564 from the National Cancer Institute, U.S. Department of Health and Human Services.

⊗ Abstract published in *Advance ACS Abstracts,* March 15, 1997.

S0006-2960(96)02957-1 CCC: $14.00

analogue, N^2-isobutyrylguanine (IbuGua),[1] in mapping the DNA binding site occupied by bleomycin during strand cleavage. The results suggest that IbuGua may be a generally useful reagent for mapping binding sites of minor groove ligands.

EXPERIMENTAL PROCEDURES

Synthesis of IbuGua-Containing Oligonucleotides. Syntheses were performed by the phosphoramidite method using a Millipore Expedite DNA synthesizer and Expedite reagents, including the modified capping Reagent A (*tert*-butylphenoxyacetic anhydride). The fifth nucleotide precursor channel was loaded with N^2-isobutyryldeoxyguanosine β-cyanoethyl phosphoramidite, a more conventional guanine precursor, in place of the Expedite reagent, and this precursor was used for just one of the G's in the sequence (the Expedite reagents are characterized by more labile protecting groups, such as N^2-*tert*-butylphenoxyacetyl in the case of the guanine precursor). Following elution of each oligonucleotide from the column, the eluate was incubated for 4 h at 22 °C, and the oligonucleotide was then immediately precipitated with 10 volumes of isobutanol. The precipitate was dissolved in 0.5 mL of H_2O and stored at −20 °C. In early experiments, similar syntheses were performed with Applied Biosystems FOD Reagents (no longer available) except that the samples were lyophilized instead of isobutanol-precipitated.

To separate IbuGua-containing oligonucleotides from those that had been completely deblocked, the samples were loaded on a Rainin 4.6 × 250 mm Microsorb C_{18} column and eluted at 1 mL/min with a 60 min linear gradient of 9 to 12% acetonitrile in H_2O, containing 0.1 M triethylammonium acetate at pH 7. Each eluted sample was lyophilized, dissolved in 0.2 mL of H_2O, and stored at −20 °C. IbuGua-containing oligonucleotides were apparently stable for at least several months.

To determine the base composition, 3 μg of each oligonucleotide was digested with 0.2 unit of snake venom phosphodiesterase and 0.8 unit of bacterial alkaline phosphatase (Pharmacia) for 16 h at 37 °C in 0.1 mL of 33 mM Tris-HCl (pH 7.5)/16 mM $MgCl_2$/1 mM $ZnCl_2$. The digestion products were analyzed by HPLC as above, except with an elution profile consisting of a 20 min wash at 5% acetonitrile followed by a 40 min gradient of 5 to 21% acetonitrile. An authentic standard of N^2-isobutyryldeoxyguanosine was obtained from Aldrich Chemicals.

Bleomycin Treatment of Oligomers. Bleomycin A_2 was a generous gift of W. Bradner (Bristol Laboratories). Peplomycin was obtained from N. R. Lomax (Drug Synthesis & Chemistry Branch, Developmental Therapeutics Program, Division of Cancer Treatment, National Cancer Institute). To prepare Fe(III) complexes, a single large crystal of ferric ammonium sulfate 12-hydrate was dissolved in 1 mM HCl at a concentration of 2 mM, and immediately upon dissolution, an aliquot was added to an equal volume of 2 mM bleomycin A_2 or peplomycin (ϵ_{290} = 14 100) in H_2O. After 5 min at 22 °C, the sample was frozen at −20 °C.

Oligonucleotides were 5′-^{32}P-end-labeled with [γ-^{32}P]ATP (3000 Ci/mmol, New England Nuclear) and T4 polynucleotide kinase according to standard procedures. Prior to bleomycin treatment, each labeled DNA strand was annealed to an excess of its complement; samples containing 0.4 and 0.8 μg/mL labeled and unlabeled oligomer in 0.1 M NaCl/10 mM Hepes−NaOH (pH 8) were heated in a 50 °C water bath for 10 min and then sequentially held at 37 °C (air incubator), 22 °C (ambient), and 4 °C (cold room) for 15 min each. All subsequent manipulations were performed on ice.

Bleomycin−DNA reactions contained 50 μg/mL calf thymus DNA, <1 μg/mL labeled duplex oligomer, and 2.5−10 μM Fe(III)·bleomycin [or Fe(III)·peplomycin] in 15 μL of 1 mM H_2O_2/0.1 M NaCl/10 mM Hepes−NaOH at pH 8. Following incubation for 1 h on ice, the DNA was ethanol-precipitated, dissolved in formamide containing 20 mM EDTA at pH 8, and immediately loaded onto a 24% denaturing polyacrylamide sequencing gel. The gels (40 × 30 × 0.8 cm) were run for 6 h at 50 W, covered with cellophane wrap, and subjected to quantitative phosphorimage analysis. Samples in which 20−50% of the labeled DNA strand was broken were used for analysis of cleavage frequency. Cleavage was calculated as the phosphorimage intensity of each band divided by the total intensity at and above that band on the gel. Exclusion of any faster-migrating radioactivity from the denominator in these calculations takes account of the fact that cleavage at a particular site will not be detected in any individual molecules which have sustained an additional break closer to the labeled end.

Modeling. Modeling was carried out using the Sybyl program (Tripos Associates) on a Silicon Graphics workstation. Except as indicated, energy minimizations were performed by the steepest descent method using the Tripos force field and Gasteiger−Hückel charges. In some cases, the structures were then solvated with one layer of H_2O and subjected to minimization by the conjugate gradient method. This particular sequence of minimizations was chosen because of its success in predicting the structure of an adriamycin−DNA complex (Fornari et al., 1993).

To evaluate the effect of IbuGua substitution on DNA structure, isobutyric acid was first minimized and then manually attached to the N-2 position of G in GGGGCAAA·TTTGCCCC. Although there are three rotatable bonds between C-2 of guanine and C-α of the isobutyryl group, the choice of rotamers was severely limited due to steric interference with the walls of the minor groove. Each plausible conformation was energy-minimized with the DNA kept rigid, and then the DNA, except for the terminal base pairs, was released and the entire structure again minimized by the steepest descent method for 5000 iterations. The structure was solvated and then minimized by the conjugate gradient method. The minimization was terminated at 500 iterations, as more extensive minimization tended to gradually introduce significant deviations from normal B-DNA structure in both the unsubstituted and substituted duplexes.

To construct a model of an intercalated bleomycin−DNA complex, the crystal structure of the $(adriamycin)_2$−d(CGATCG)$_2$ complex (Frederick et al., 1990) was obtained from the Brookhaven data base. In this model structure, intercalation occurs at the CG steps on both ends of the duplex. Thus, to produce a duplex with a central intercalation site, adriamycin was deleted and two copies of the d(ATCG)·d(CGAT) portion of the structure were placed head to head, with the two empty intercalation sites superimposed. Overlapping base pairs were then eliminated, and the two

[1] Abbreviations: IbuGua or Ibu-G, N^2-isobutyrylguanine; HPLC, high-pressure liquid chromatography; rms, root-mean-squared.

sugar−phosphate backbones were linked, to produce a $d(ATCGAT)_2$ duplex. The sequence of bases was altered using the Mutate function of Sybyl, and two G·C base pairs of B-DNA were added to one end, to give a GGG-GCAAA·TTTGCCCC duplex with an intercalation site between the two underlined base pairs.

Bleomycin A_2 was constructed manually in Sybyl, and the metal chelation site was configured according to the constraints suggested by Wu et al. (1996a). The carbohydrate moieties were removed, and the bithiazole was placed in the *trans* form. Following an initial minimization, the structure was placed in the general configuration suggested by Wu et al. (1996a), by manipulating the rotatable bonds in the peptide chain. This structure was manually docked into the intercalation site in the GGGGCAAA·TTTGCCCC duplex, and the rotatable bonds were further adjusted to allow placement of the bleomycin pyrimidine within hydrogen bonding distance of the guanine 5′ to the cleavage site (G in GGGGCAAA). To maintain this hydrogen bonding, the distance between the N-3 of guanine and the 4-amino group of the pyrimidine and the distance between the 2-amino group of guanine and N-3 of the pyrimidine were each set to 2.2 Å, with a force constant of 50 kcal/Å. The two terminal base pairs were then fixed in position, and the remaining bleomycin−DNA complex was minimized as above, except that charges on the chelated cobalt atom and on the dimethylsulfonium sulfur were fixed at +3 and +1, respectively. The structure was then solvated; the terminal base pairs were released, and the entire structure was repeatedly minimized by the conjugate gradient method, until the minimization traversed 100 consecutive iterations with a cumulative energy change of less than 1 kcal/mol.

To assess the degree to which IbuGua substitution would disrupt this model structure, the IbuGua moiety was extracted from the GGG(Ibu-G)CAAA duplex described above. The guanine portion of this structure was superimposed on each guanine in the sequence, while keeping the entire IbuGua moiety rigid, in order to position the isobutyryl group in precisely the same relative orientation as in the minimized GGG(Ibu-G)CAAA duplex. The bleomycin−DNA complex was desolvated, and the positioned isobutyryl group was attached to the appropriate guanine. The constraints related to hydrogen bonding of bleomycin to DNA were released and the terminal base pairs fixed in position, and the structure was energy-minimized for 1000 iterations by the steepest descent method. The root-mean-squared (rms) change in the coordinates of bleomycin·Co(III)·OOH^- only was then computed using the Match function.

RESULTS

Characterization of DNA Substituted with IbuGua. In order to synthesize DNA oligomers containing IbuGua at a particular position, the synthesis was performed with rapid-deprotection Expedite reagents, except that a standard isobutyryl-protected guanine precursor (Figure 1) was used at one position in the sequence. Following a short alkaline hydrolysis sufficient to remove nearly all the more labile protecting groups, each synthesized oligomer was subjected to HPLC. The majority of the DNA eluted at the same position as fully deprotected oligomer, while 20−40% eluted significantly later in a gradient of increasing hydrophobicity, consistent with the presence of an isobutyryl group (Figure 2A). To verify the structure of these modified oligomers, each was digested to nucleosides with snake venom phosphodiesterase and alkaline phosphatase, and the products were analyzed by HPLC. Each of the early-eluting oligomers was found to contain only the normal DNA nucleosides in the expected proportions (Figure 2B). Each of the late-eluting oligomers contained an additional species which comigrated with authentic N^2-isobutyryldeoxyguanosine, and a commensurately lesser amount of deoxyguanosine (Figure 2C). Thus, it is inferred that each modified oligomer was in fact substituted with a single IbuGua in the desired position.

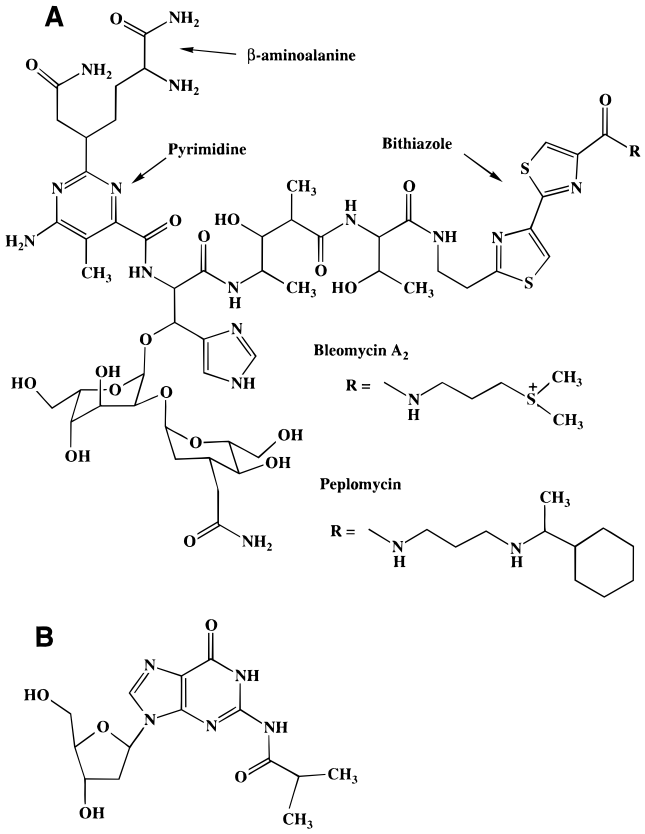

FIGURE 1: Structures of metal-free bleomycin (A) and N^2-isobutyryldeoxyguanosine (B).

When the modified and unmodified oligomers were 5′-end-labeled with ^{32}P, electrophoresis on sequencing gels revealed a major radiolabeled band for each. Again, the early-eluting HPLC peaks all had the same mobility as a completely deprotected oligomer, while the IbuGua-containing oligomers had mobility about 5% slower. Since numerous unidentified contaminants were also present (not shown), all radiolabeled oligomers were purified by preparative polyacrylamide gel electrophoresis, followed by a second cycle of HPLC, before use.

Effect of IbuGua Substitution on Bleomycin-Induced DNA Cleavage. As shown previously, bleomycin induces DNA double-strand breaks with predominantly either no stagger or a one-base 5′ stagger between the breaks in complementary strands (Povirk et al., 1989; Absalon et al., 1995a). Each primary break occurs at a G-Py sequence, and the exact position of the secondary break is determined by a hierarchy of sequence-dependent selection rules. The oligonucleotide duplex used for determination of the effect of minor groove blockage on DNA cleavage, i.e., $T_1G_2C_3T_4G_5G_6G_7G_8C_9$-$A_{10}A_{11}A_{12}C_{13}C_{14}A_{15}G_{16}C_{17}$ annealed to $G_{18}C_{19}T_{20}G_{21}G_{22}$-

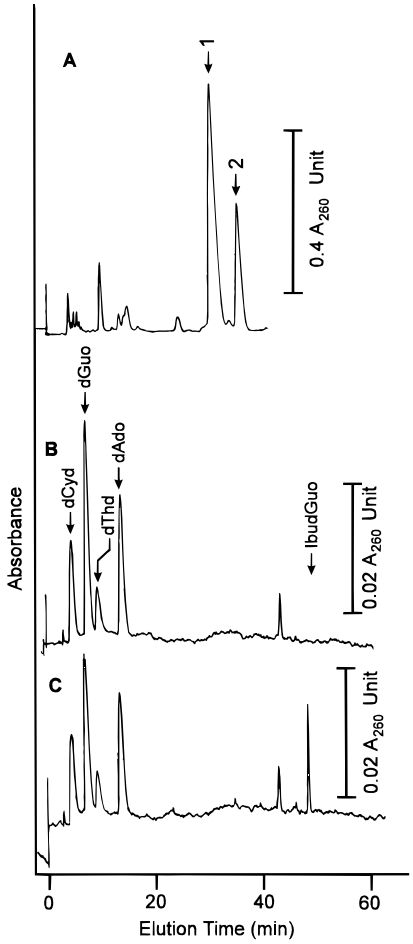

FIGURE 2: Characterization of an IbuGua-substituted oligomer. (A) Ultraviolet absorbance elution profile (260 nm) showing separation of fully deprotected (peak 1) and IbuGua-substituted (peak 2) oligomers by HPLC following phosphoramidite synthesis. (B and C) Nucleoside composition of peak 1 (B) or peak 2 (C) from the separation shown in part A, as determined by HPLC analysis following digestion with snake venom phosphodiesterase and alkaline phosphatase. The peak at 42 min is a solvent artifact which was present even when no sample was injected. Data shown are for the oligomer substituted at G_7; similar results were obtained for the other substituted oligomers. IbudGuo = N^2-isobutyryldeoxyguanosine.

$T_{23}T_{24}T_{25}G_{26}C_{27}C_{28}C_{29}C_{30}A_{31}G_{32}C_{33}A_{34}$, was based on a sequence from the *lacI* gene. Studies with a longer fragment containing this sequence (Povirk et al., 1989) indicated the presence of two major sites of double-strand cleavage, one involving primary cleavage at C_9 in the top strand and secondary cleavage on a one-base 5′ stagger at T_{25} in the bottom strand and the other involving primary cleavage at C_{27} in the bottom strand and secondary cleavage directly opposite, at G_8 in the top strand (see Figure 5). As shown in Figure 3 (top strand) and Figure 4 (bottom strand), bleomycin or peplomycin treatment of the 17-mer duplex confirmed cleavage at all of these sites, with stronger cleavage at each primary site. There was also weak cleavage at T_{23} in the bottom strand, with associated secondary cleavage at A_{12}. In single-stranded DNA, there was some cleavage, on the bottom strand only, at C_{33}, presumably due to self-annealing.

Figures 3 and 4 also show representative assays of the effects of IbuGua substitution at certain positions in the fragment on bleomycin-induced DNA cleavage, and these effects are summarized in Figure 5. Considering first the

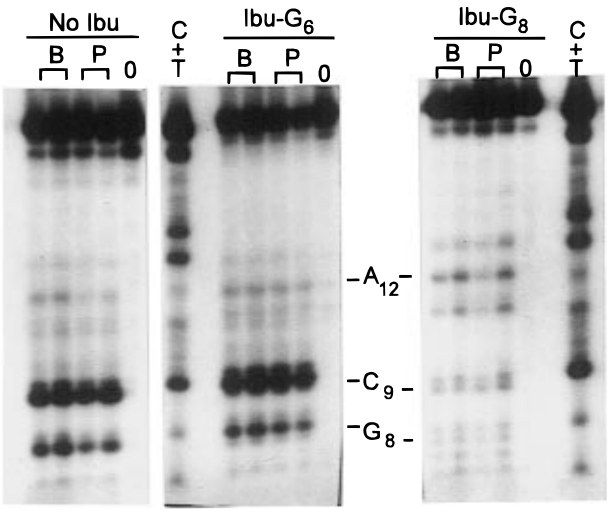

FIGURE 3: Effect of IbuGua substitution on cleavage of 5′-^{32}P-end-labeled $T_1G_2C_3T_4G_5G_6G_7G_8C_9A_{10}A_{11}A_{12}C_{13}C_{14}A_{15}G_{16}C_{17}$ by bleomycin or peplomycin. Oligomers substituted with IbuGua as indicated were annealed to a complementary oligomer and treated with 2.5 μM Fe(III)·bleomycin (B) or Fe(III)·peplomycin (P), and the cleavage products were analyzed on a denaturing gel. The C+T lanes are Maxam−Gilbert markers. Note that cleavage at G_8 and at C_9 yields a doublet in each case, presumably representing fragments with 3′-phosphoglycolate and 3′-phosphate termini (Steighner & Povirk, 1990). For unsubstituted and G_6-substituted substrates, the faster-migrating 3′-phosphoglycolate band predominates, but for the G_8-substituted substrate, the two bands have comparable intensity.

primary cleavage sites, cleavage at C_9 was reduced 12−14-fold by IbuGua substitution immediately 5′ at G_8, and 4−5-fold by IbuGua substitution two bases 5′ at G_7; in addition, nearly half of the residual breaks in the G_8-substituted substrate appeared to have 3′-phosphate termini rather than the 3′-phosphoglycolate termini characteristic of bleomycin-induced cleavage (see Figure 3). Primary cleavage at C_{27} was reduced about 7-fold by IbuGua substitution directly opposite at G_8 but was completely unaffected by substitution one base 3′ at G_7. Substitution at G_5 or G_6 had no effect on cleavage at either primary site. Thus, cleavage at primary sites appears to be substantially blocked by IbuGua substitution at any of three base pairs: the base pair that is actually the target and two additional base pairs in the 5′ direction with respect to the strand containing the target nucleotide.

Inhibition of cleavage at secondary sites followed a more complex pattern. Secondary cleavage at G_8 was reduced more than 20-fold when G_8 itself was substituted and was reduced about 10-fold by substitution one base 5′ at G_7, even though that substitution had no effect on cleavage at the corresponding primary site, C_{27}. Most strikingly, however, secondary cleavage at T_{25} was decreased 4-fold by IbuGua substitution two bases 3′ at G_8, a distinctly different pattern than was seen for the primary site C_{27}. Indeed, substitution at G_7 also inhibited cleavage at T_{25} (about 2-fold) even though it had no effect on cleavage at C_{27}, which is two bases closer to the substitution. The most likely explanation of these data is that cleavage at each secondary site can only occur following cleavage at the corresponding primary site and that inhibition of secondary cleavage (in this case at T_{25}) is an indirect result of inhibition of primary cleavage (in this case at C_9). Curiously, however, secondary cleavage was in both cases inhibited less than primary cleavage (see Discussion).

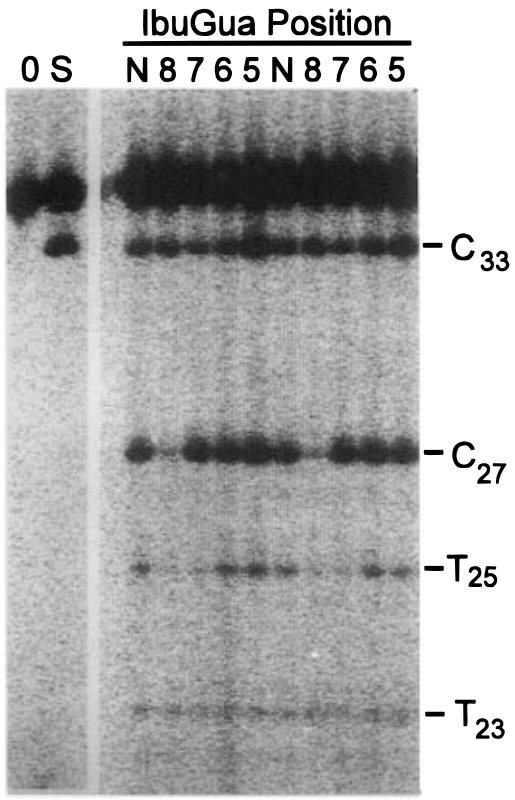

FIGURE 4: Effect of IbuGua substitution on cleavage of 5′-^{32}P-end-labeled $G_{18}C_{19}T_{20}G_{21}G_{22}T_{23}T_{24}T_{25}G_{26}C_{27}C_{28}C_{29}C_{30}A_{31}G_{32}C_{33}A_{34}$ by bleomycin. The oligomer was annealed to a complement substituted with IbuGua at the indicated positions (see Figure 5 for numbering of positions), and following treatment with 5 μM Fe(III)·bleomycin, the cleavage products were analyzed on a denaturing gel. N indicates no IbuGua substitution, 0 no bleomycin, and S a bleomycin-treated single-stranded fragment. Cleavage positions were verified by comparison with Maxam−Gilbert sequencing markers (not shown).

Peplomycin has a longer terminal amine than bleomycin A_2 (Figure 1). Thus, if the terminal amine lies extended along the interior or the minor groove, it would be expected that the binding site of peplomycin might be ~1 bp larger than that of bleomycin. However, the data showed no detectable differences between these two analogues in the inhibition of cleavage by IbuGua substitution at any position. This result was somewhat surprising but is consistent with a recent proposal that the terminal amine actually passes through the DNA helix and protrudes into the major groove (Absalon et al., 1995b).

Molecular Modeling. Computer graphics modeling was employed in an attempt to determine the structural basis for the effects of IbuGua substitution on cleavage. Modeling of the isobutyryl adduct itself (attached to B-DNA at G in the sequence GGGGCAAA) revealed that the adduct could be easily accommodated in the minor groove without significant distortion of DNA structure (Figure 6). Among the many IbuGua conformations examined, the lowest potential energy following minimization was obtained from one in which the remaining hydrogen on guanine N-2 retained normal Watson−Crick hydrogen bonding, and the isobutyryl carbonyl was nearly coplanar with the guanine base, with the oxygen pointing toward the backbone of the adducted DNA strand (approximately as drawn in Figure 1). The isobutyryl carbonyl−C-α bond was thus directed back toward the center of the minor groove. Rotation about this bond determines the orientation of the two methyl groups, and van der Waals interactions with the walls of the groove resulted in a strong tendency for the methyls to align along the groove, rather than transverse to it. A slightly lower energy was obtained with the bond rotated such that the two methyls faced toward the adducted strand. In this orientation, the minimized isobutyryl group itself had a slightly negative calculated potential energy, even with the DNA kept rigid and no solvent added. Minimized structures of IbuGua-substituted and unsubstituted GGGGCAAA·TTTGCCCC oligonucleotide duplexes (Figure 6) were virtually superimposable. Thus, quite fortuitously, the isobutyryl group appeared to be of nearly optimal size and shape to effectively block access to the minor groove at a well-defined position, but without significantly disturbing DNA secondary structure. NMR studies of a slightly bulkier styrene oxide adduct on guanine N-2 have also indicated only minor, highly localized perturbations of B-DNA structure (Zegar et al., 1996).

On the basis of NMR data, two research groups have recently proposed quite similar models for the binding of bleomycin·Co(III)·OOH^- to oligonucleotide duplexes (Mao et al., 1996; Wu et al., 1996a). In these models, the overall conformation of free bleomycin·Co(III)·OOH^-, with the bithiazole folded "below" the chelation complex (i.e., on the same side as the peroxide anion ligand), is preserved upon DNA binding. The bithiazole, in the *trans* conformation, is transversely intercalated immediately 3′ to the nucleotide attacked (i.e., a line connecting the two thiazole rings is roughly perpendicular to a line connecting the two DNA backbones). In the more detailed model proposed by Wu et al. (1996a), the terminal amine protrudes into the major groove, and the bleomycin pyrimidine moiety, which is a Co(III) ligand, is hydrogen bonded to the guanine immediately 5′ to the nucleotide attacked, thus conferring the G-Py specificity of DNA cleavage.

Since the proposed transverse intercalation of the bithiazole is similar to that of adriamycin, and the unwinding angle is also similar (Povirk et al., 1979), the starting point for the modeling of the bleomycin−DNA complex was incorporation of the DNA−adriamycin intercalation site from the X-ray crystallography of Frederick et al. (1990) into the bleomycin target 8-mer GGGGCAAA·TTTGCCCC, with intercalation between the two underlined base pairs. The Co(III) chelation site in the bleomycin·Co(III)·OOH^- complex was constructed using the constraints suggested by Wu et al. (1996a). To simplify the computations, the carbohydrate moieties, which do not significantly contribute to the specificity of DNA cleavage (Sugiura et al., 1983), were removed. The full deglycobleomycin·Co(III)·OOH^- complex was docked manually into the intercalation site in the general conformation described by Wu et al. (1996b). Following an initial energy minimization, the structure was solvated and again energy-minimized. In the absence of any additional constraints, the chelation complex tended to very gradually drift out from the minor groove during minimization, with eventual loss of hydrogen bonding between the bleomycin pyrimidine and DNA. Therefore, additional constraints were introduced in order to maintain these hydrogen bonds. With these constraints, the overall structure was quite stable through extensive minimization; in particular, the peroxide anion, which is the analogue of the oxygen that would be activated during DNA cleavage by iron−bleomycin, remained strategically positioned near its abstraction target, C-4′ of C in the GGGGCAAA sequence (asterisk

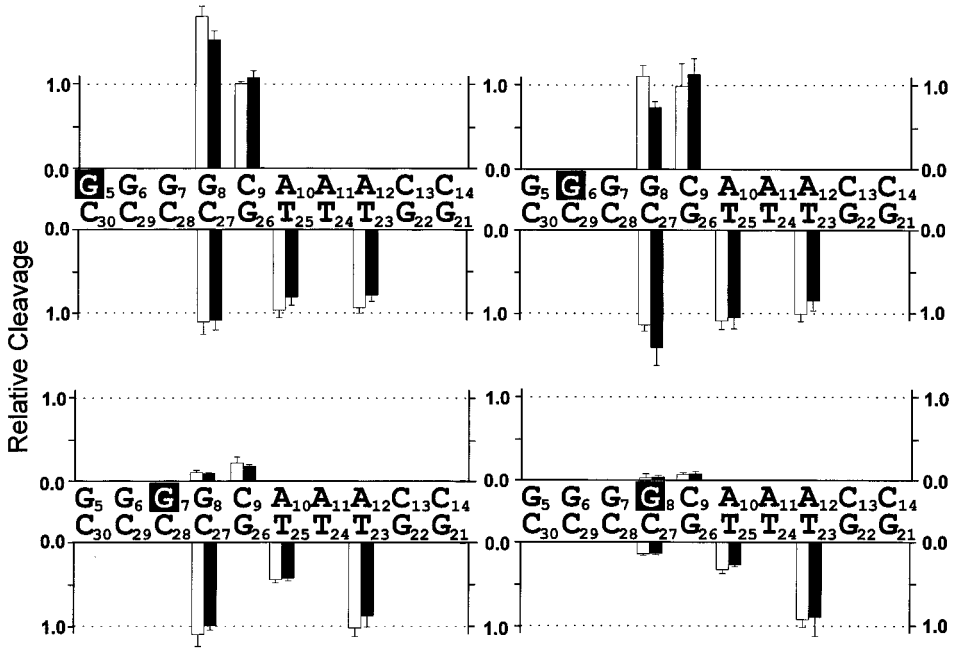

FIGURE 5: Quantitative analysis of the effect of IbuGua substitution at various positions on site-specific DNA cleavage by bleomycin or peplomycin. The position of the substitution is indicated by white-on-black lettering. Open and closed bars show the average cleavage at each site by bleomycin A_2 and peplomycin, respectively, normalized to cleavage at that same site in the unmodified duplex. Each bar is the average of three to six determinations (±S.D.), as determined from phosphorimage analysis of denaturing gels (see Figures 3 and 4).

in Figure 7A−D). Reattachment of the carbohydrate moieties to the energy-minimized structure, followed by additional minimization, did not detectably affect the conformation of the complex; indeed, it appeared highly unlikely that the sugars could make any contact with DNA at all, given their attachment to the outermost portion of the metal-binding domain (data not shown).

To determine whether IbuGua moieties in the DNA duplex would interfere with the positioning of deglycobleomycin·Co(III)·OOH^- in the model structure, an isobutyryl group was attached to each guanine in turn, in the conformation predicted from the modeling of GGG(Ibu-G)CAAA; to assess the effect of substitution immediately 3′ to the cleavage site, it was necessary to change the A·T base pair at that position to a C·G base pair.

As shown in Figure 7B, an IbuGua substitution immediately 5′ to the cleavage site (where the isobutyryl group would replace one of the hydrogens involved in hydrogen bonding to the bleomycin pyrimidine) resulted in prohibitively close contacts with the bleomycin pyrimidine. Upon minimization of this structure (not shown), the pyrimidine moiety was forced up and away from the guanine. Substitution directly at the base pair attacked (i.e., at G opposite C in the GGGGCAAA sequence; Figure 7C) resulted in similarly close contacts, primarily between the isobutyryl methyl groups and the bleomycin peptide chain as it emerges from the intercalated bithiazole. When this structure was minimized, this portion of the peptide chain was forced down, away from the chelation site, in a highly strained configuration. For either of the initial substituted structures, space-filling models (not shown) indicated severe van del Waals overlap, and the initial energies were $>10^8$ kcal/mol. In each case, minimization of the isobutyryl group, with both DNA and bleomycin held rigid, resulted in severe distortion, with final energies of several hundred kilocalories per mole in the isobutyryl group alone.

An isobutyryl adduct two bases 5′ to the cleavage site (Figure 7A) resulted in slight overlap with the bleomycin metal-binding domain, while an adduct immediately 3′ to the cleavage site just barely contacted two hydrogens of the bleomycin peptide chain (Figure 7D). Isobutyryl adducts at other positions farther 3′ and 5′ were all well-separated from the bound bleomycin (not shown).

Figure 8B shows two quantitative measures of the degree to which IbuGua substitution at various guanines in the duplex perturbs the model DNA−bleomycin complex. The first is the rms change in the bleomycin coordinates that occurred when the entire bleomycin−DNA complex was minimized following addition of the isobutyryl group. The second is the computed potential energy of the (unsolvated) substituted complex, following a brief energy minimization. By either of these criteria, the structure was much more severely perturbed by substitution either at or immediately 5′ to the cleavage site than at other positions in the duplex. Perturbation of the model structure was considerably less for substitution two bases 5′ and one base 3′ from the cleavage site and was negligible for other positions. Thus, the modeling results were in reasonable agreement with the empirical data on site-specific cleavage, summarized in Figure 8A.

DISCUSSION

Elucidation of the nature of the complex between bleomycin and DNA has proven to be unexpectedly difficult. Early studies with Cu(II)·bleomycin, metal-free bleomycin, and a bleomycin fragment consisting of the bithiazole and terminal amine suggested a binding geometry involving intercalation of the bithiazole rings (Povirk et al., 1979; Lin & Grollman, 1981). However, there have also been some fairly compelling arguments against intercalation, including the bulkiness of the side chains linked to both ends of the bithiazole, as well as the very similar cleavage patterns

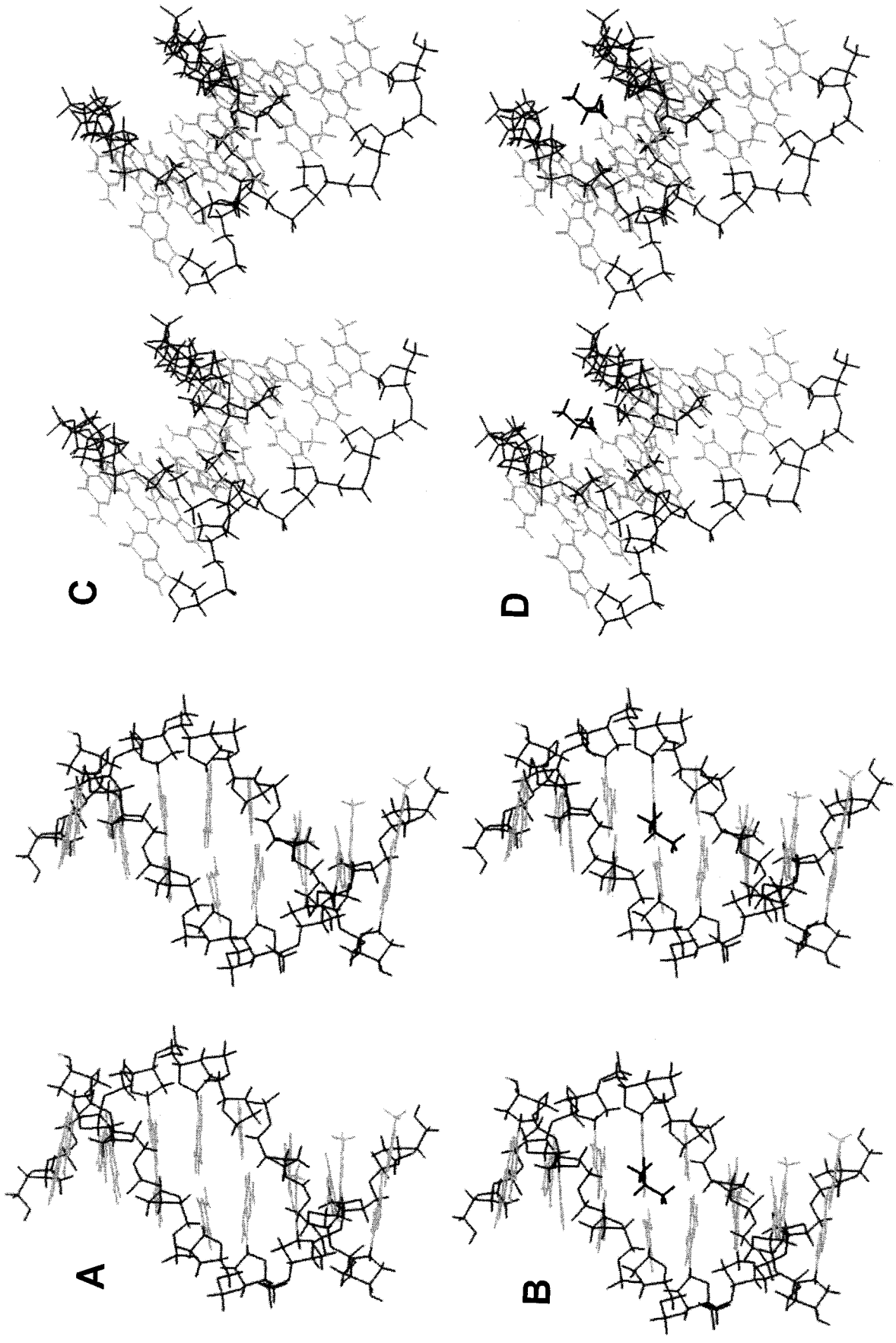

FIGURE 6: Minimized model structures (stereoview) of GGGGCAAA·TTTGCCCC (A and C) and GGG(Ibu-G)CAAA·TTTGCCCC (B and D). DNA bases and backbones are depicted in light and dark gray, respectively, and the isobutyryl group is depicted in black. In parts A and B, the helix axis is set vertically; the backbone of the IbuGua-containing strand begins at the upper left, loops in back of the helix, and then passes to the right of the adduct, reading 5′ → 3′ from top to bottom. In parts C and D, the top of the helix has been tilted back and to the left so that the line of sight passes through the minor groove at the site of the substitution. All stereoviews are in the "relaxed" mode.

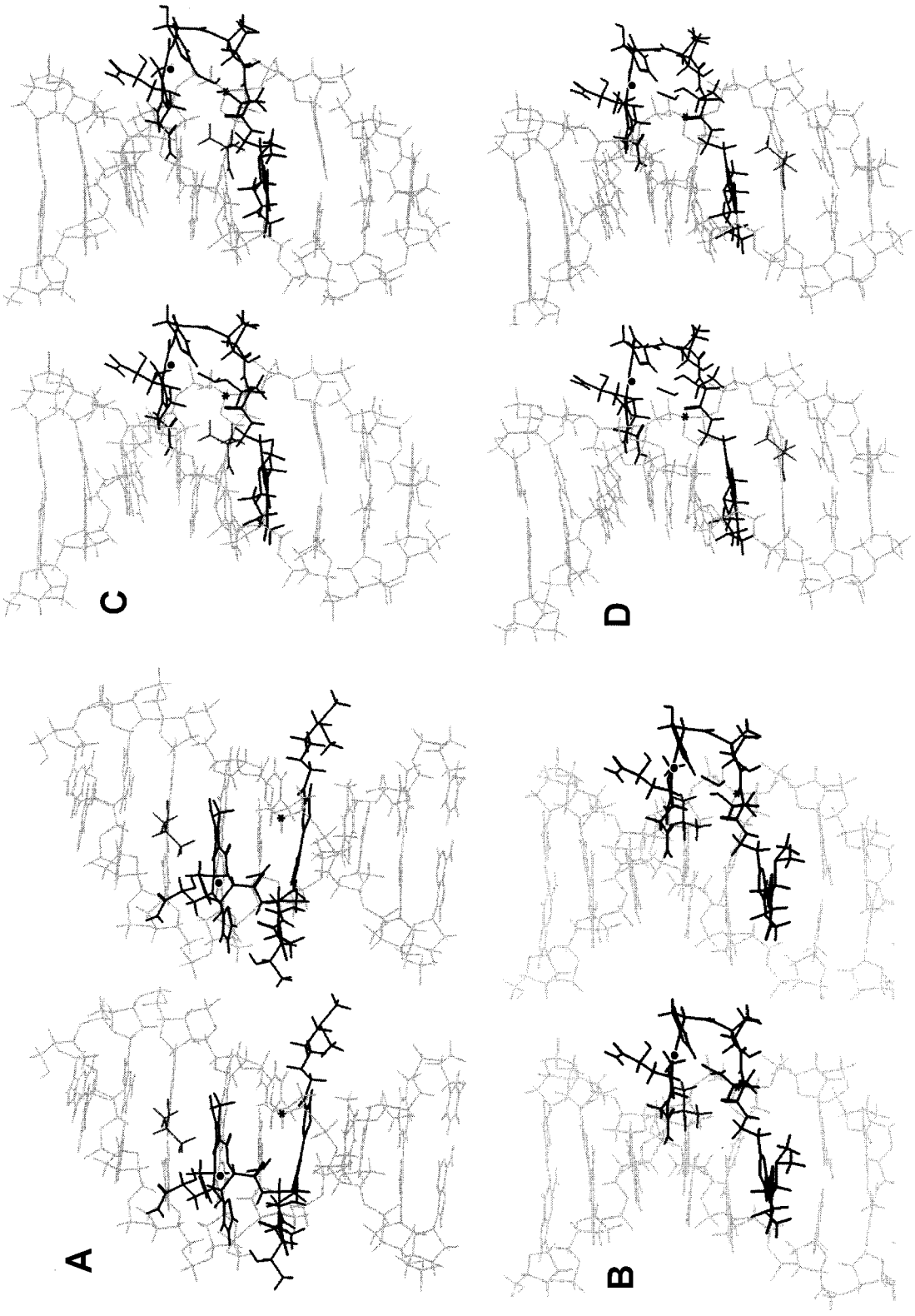

FIGURE 7: Addition of isobutyryl groups to guanines at various positions in the model structure of bleomycin•Co(III)•OOH^- bound to DNA. Bleomycin•Co(III)•OOH^- is shown in black, DNA in light gray, and the isobutyryl group in dark gray. In each case, the view is into the minor groove. The metal binding domain of bleomycin•Co(III)•OOH^- is toward the top of the figure, and the bithiazole and terminal amine are toward the bottom. The large black dot is the chelated Co(III) ion, and the β-aminoalanine and OOH^- chelating groups are directly above and below it, respectively. The strand containing the cleavage site reads 5′ → 3′ GGGGCAAA from top to bottom, with cleavage at the C. The black asterisk (*) indicates the C-4′ from which activated bleomycin would abstract hydrogen. Positions of IbuGua substitution are G in GGGGCAAA (A), G in GGGGCAAA (B), G opposite C in GGGGCAAA (C), and G opposite C in the modified sequence GGGGCCAA (D). Note the steric overlap between the isobutyryl group and the bleomycin pyrimidine [which lies just to the left of the Co(III) ion] in part B and between the isobutyryl group and the bleomycin peptide chain in part C.

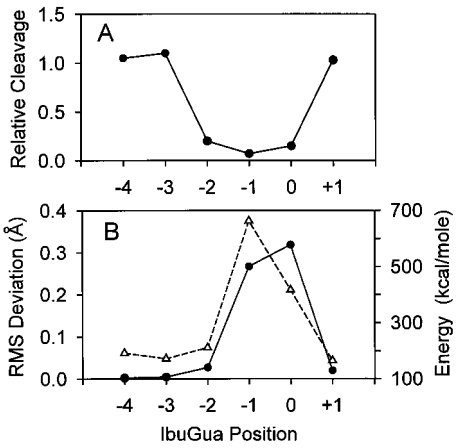

FIGURE 8: Comparison of empirical data on IbuGua-induced inhibition of DNA cleavage with the predictions of modeling studies. Panel A shows the inhibition of bleomycin-induced DNA cleavage by IbuGua substitution at various positions in the duplex with respect to the cleavage site. Cleavage inhibition for positions −4 through −1 is taken from data for cleavage at C_9, and inhibition for the 0 and +1 positions is from data for cleavage at C_{27}. Panel B shows the degree to which IbuGua substitution at each site altered the coordinates of bleomycin·Co(III)·OOH^- in the model bleomycin−DNA complex (●); following attachment of the isobutyryl group to an extensively minimized bleomycin−DNA structure, the entire structure was desolvated and again minimized, and the root-means-squared (rms) deviation of the bleomycin·Co(III)·OOH^- coordinates, before and after the final minimization, were computed. The potential energy of the final structure (△) was also computed in each case. The potential energy of the unsubstituted complex was 168 kcal/mol.

produced by the bleomycin analogue phleomycin, in which the planarity of the bithiazole is destroyed by loss of one double bond (Kross et al., 1982). Thus, nonintercalative models have been proposed in which the bithiazole binds in the minor groove, following the curvature of the groove in a manner similar to that of distamycin (Kuwahara & Sugiura, 1988; Dickerson, 1986). In this configuration, bleomycin binding can occur with little or no perturbation of DNA structure, and hydrogen bonding between the bithiazole nitrogens and the 2-amino group of guanine could potentially account for the G-Py specificity of bleomycin-induced DNA cleavage. However, several recent findings argue against such simple groove binding. First, patterns of bleomycin-induced cleavage of nucleosomal DNA are much more similar to those of intercalating molecules (e.g., neocarzinostatin) than to those of groove binders (e.g., calicheamicin) (Smith et al., 1994; Yu et al., 1994, 1995; Kuduvalli et al., 1995). Second, synthetic DNA-cleaving compounds consisting of Fe(II)·EDTA linked to a bithiazole show almost no sequence specificity (Kane et al., 1994). Third, synthetic bleomycin analogues which have rigid linkers of varying length between the bithiazole and metal-binding domains (Carter et al., 1990), or which lack the bithiazole entirely (Guajaro et al., 1993), show cleavage specificity similar to that of the drug itself. Thus, while the bithiazole likely stabilizes DNA binding, the basis of sequence specificity seems to reside in the metal-binding domain, not in the bithiazole.

Most recently, two-dimensional NMR spectra of metal−bleomycin complexes bound to defined-sequence oligonucleotides have allowed the first credible attempts at assigning the structural details of bleomycin−DNA binding. In particular, the bleomycin·Co(III)·OOH^- complex (also referred to as the green or form I cobalt complex), when bound to oligonucleotide duplexes, consistently shows large upfield shifts of the bithiazole ring hydrogens, strongly suggesting intercalation (Mao et al., 1996; Wu et al., 1994). Moreover, on the basis of the loss of NOE coupling between specific DNA bases, both Mao et al. (1996) and Wu et al. (1994, 1996a,b) have concluded that intercalation occurs immediately 3′ to the cleavage site (e.g., between the two C's in GCC, where the underlined C is cleaved). Using additional NMR-derived distance constraints, Wu et al. (1996b) have proposed a detailed model in which the 4-amino group and N-3 of the pyrimidine in the bleomycin metal-binding domain are hydrogen-bonded to the N-3 and 2-amino group of the guanine immediately 5′ to the cleavage site, thus conferring G-Py specificity. In this model, the flexible peptide chain loops along the minor groove in the 3′ direction (with respect to the strand sustaining cleavage), and the bithiazole is transversely intercalated with the terminal amine protruding into the major groove (as in Figure 7). Although Zn(II)·bleomycin (Manderville et al., 1994) and the peroxide-free form of Co(III)·bleomycin (Mao et al., 1996) appear to bind to oligonucleotide duplexes without intercalation, bleomycin·Co(III)·OOH^- merits special consideration because it effects a light-dependent DNA cleavage reaction with sequence specificity very similar to that of activated iron−bleomycin (Nightingale & Fox, 1994). Therefore, we have taken an intercalated complex as the starting point for modeling the effects of minor groove blockage on bleomycin−DNA binding.

As shown in Figure 7, this model predicts the effects of IbuGua substitution on site-specific DNA cleavage with reasonable accuracy, consistent with the proposal that such cleavage is effected by an activated iron−bleomycin species that is bound to DNA with a geometry similar to that described for bleomycin·Co(III)·OOH^-. In particular, the abrupt loss of inhibition, as the IbuGua substitution is moved from the 0 position (the G directly opposite the cleavage site) to the +1 position, is consistent with intercalation of the bithiazole across the helix immediately 3′ to the cleavage site, with the terminal amine protruding into the major groove. If the terminal amine were to loop back into the minor groove, significant steric interference from isobutyryl groups on either side of the intercalation site would have been expected. The finding that the effects of site-specific minor groove blockage are virtually the same for bleomycin as for peplomycin also suggests that the terminal amine does not occupy the minor groove. The only deviation of the empirical data from the modeling is that the observed inhibition resulting from IbuGua substitution at the −2 position is somewhat greater than might be expected from the very slight overlap seen in the model structure (Figure 7A). However, the insertion of the bleomycin metal-binding domain into the minor groove requires some perturbation of both the DNA and bleomycin structure, and it is apparent from the model structure that very small differences in the orientation of that domain could significantly change the extent of its overlap with an isobutyryl group at the −2 position. It is also notable that cleavage at a secondary site (G_8), unlike cleavage at a primary site, is not inhibited by an IbuGua substitution two bases 5′ to that site (Figure 5). Since primary and secondary cleavage events both involve stereospecific attack at C-4′, it is likely that the orientation of the bleomycin metal-binding domain with respect to the

primary and secondary sites is very similar. Thus, the fact that IbuGua substitution inhibits one and not the other again suggests that such an IbuGua substitution may lie just at the edge of the bleomycin metal-binding domain.

On the basis of the kinetics, sequence specificity, and product distribution at sites of bleomycin-induced bistranded DNA damage, we previously proposed a model of double-strand cleavage in which a single molecule of bleomycin first effects cleavage at a primary (G-Py) site and then undergoes reactivation and conformational rearrangement to effect cleavage at a secondary site in the complementary strand (Steighner & Povirk, 1990; Povirk et al., 1989). In this model, the primary cleavage event is a necessary but not sufficient condition for the secondary cleavage event, and the position of primary cleavage is the principal determinant of the position of secondary cleavage. Consistent with the model, cleavage at a predicted secondary site (T_{25}) was inhibited by all substitutions which suppressed cleavage at the corresponding primary site (C_9), even when those substitutions were several bases away from the secondary site. These results are corroborated by those of Absalon et al. (1995b), which showed that deuterium substitution at the C-4′ position of a primary site inhibited cleavage at both the primary site and the corresponding secondary site. In both experimental systems, however, inhibition was consistently greater at the primary than at the secondary site. This result is at odds with a simple model in which each primary cleavage event has a certain probability of leading to a secondary cleavage event, and it implies that either there was some *bona fide* single-strand cleavage at the secondary site in the modified substrates or the ratio of double- to single-strand breaks was greater in the modified than in the unmodified substrates. Unfortunately, neither experimental system can clearly distinguish between these alternatives, and thus, the basis of this apparent anomaly in the data remains to be determined. In a structural sense, however, it is easy to envision the metal-binding domain swiveling across the minor groove from the primary to the secondary cleavage site, using the intercalated bithiazole as an anchor and the flexible peptide chain as a tether (see Figure 7).

The finding that the inhibitory effect of isobutyryl substitution on cleavage is so highly localized suggests that this adduct has little or no effect on the secondary structure of neighboring DNA base pairs. These results agree with the modeling studies, which predict that an isobutyryl adduct will effectively block the minor groove, but can be easily accommodated without distortion of the groove. Thus, site-specific IbuGua substitution may provide a general method for mapping the binding sites of minor groove ligands, applicable to any binding event for which a functional assay is available. As shown by the present results, this method may be particularly useful in cases where the ligand−DNA complexes are too unstable or short-lived to permit direct physical−chemical studies.

ACKNOWLEDGMENT

We thank Bettye L. Smith and Thomas Reynolds for help with the synthesis and analysis of modified oligonucleotides, Maria Gilardi for technical assistance, Gwen Bauer and Frank Fornari for helpful advice, Don Abraham for use of his computer graphics facilities, and Richard Moran and Mary Peek for editorial suggestions.

REFERENCES

Absalon, M. J., Kozarich, J. W., & Stubbe, J. (1995a) *Biochemistry 34*, 2065.

Absalon, M. J., Wu, W., Kozarich, J. W., & Stubbe, J. (1995b) *Biochemistry 34*, 2076.

Burger, R. M., Peisach, J., & Horwitz, S. B. (1981) *J. Biol. Chem. 256*, 11636.

Carter, B. J., Murty, V. S., Reddy, K. S., Wang, S. N., & Hecht, S. M. (1990) *J. Biol. Chem. 265*, 4193.

Dickerson, R. E. (1986) in *Mechanisms of DNA Damage and Repair. Implications for Carcinogenesis and Risk Assessment in Basic Life Sciences* (Simic, M. G., & Grossman, L., Eds.) pp 245−255, Plenum, New York.

Fornari, F. A., Gewirtz, D. A., Bauer, G. B., Abraham, D., & Kellogg, G. E. (1993) *Biophys. J. 64*, A284.

Frederick, C. A., Williams, L. D., Ughetto, G., van der Marel, G. A., van Boom, J. H., Rich, A., & Wang, A. H. (1990) *Biochemistry 29*, 2538.

Guajaro, R. J., Husdon, S. E., Brown, S. J., & Mascharak, P. K. (1993) *J. Am. Chem. Soc. 115*, 7971.

Hecht, S. M. (1986) *Accs. Chem. Res. 19*, 383.

Kane, S. A., Natrajan, A., & Hecht, S. M. (1994) *J. Biol. Chem. 269*, 10899.

Kross, J., Henner, W. D., Hecht, S. M., & Haseltine, W. A. (1982) *Biochemistry 21*, 4310.

Kuduvalli, P. N., Townsend, C. A., & Tullius, T. D. (1995) *Biochemistry 34*, 3899.

Kuramochi, H., Takahashi, K., Takita, T., & Umezawa, H. (1981) *J. Antibiot. 34*, 576.

Kuwahara, J., & Sugiura, Y. (1988) *Proc. Natl. Acad. Sci. U.S.A. 85*, 2459.

Lin, S. Y., & Grollman, A. P. (1981) *Biochemistry 20*, 7589.

Manderville, R. A., Ellena, J. F., & Hecht, S. M. (1994) *J. Am. Chem. Soc. 116*, 10851.

Mao, Q., Fulmer, P., Li, W., DeRose, E. F., & Petering, D. H. (1996) *J. Biol. Chem. 271*, 6185.

Nightingale, K. P., & Fox, K. R. (1994) *Eur. J. Biochem. 220*, 173.

Povirk, L. F., Hogan, M., & Dattagupta, N. (1979) *Biochemistry 18*, 96.

Povirk, L. F., Hogan, M., Dattagupta, N., & Buechner, M. (1981) *Biochemistry 20*, 664.

Povirk, L. F., Han, Y.-H., & Steighner, R. J. (1989) *Biochemistry 28*, 8508.

Smith, B. L., Bauer, G., & Povirk, L. F. (1994) *J. Biol. Chem. 258*, 30587.

Steighner, R. J., & Povirk, L. F. (1990) *Proc. Natl. Acad. Sci. U.S.A. 87*, 8350.

Stubbe, J., & Kozarich, J. (1987) *Chem. Rev. 87*, 1107.

Sugiura, Y., Suzuki, T., Otsuka, M., Kobayashi, S., Ohno, M., Takita, T., & Umezawa, H. (1983) *J. Biol. Chem. 258*, 1329.

Wu, W., Vanderwall, D. E., Stubbe, J., Kozarich, J. W., & Turner, C. J. (1994) *J. Am. Chem. Soc. 116*, 10843.

Wu, W., Vanderwall, D. E., Lui, S. M., Tang, X.-J., Turner, C. J., Kozarich, J. W., & Stubbe, J. (1996a) *J. Am. Chem. Soc. 118*, 1268.

Wu, W., Vanderwall, D. E., Turner, C. J., Kozarich, J. W., & Stubbe, J. (1996b) *J. Am. Chem. Soc. 118*, 1281.

Yu, L., Goldberg, I. H., & Dedon, P. C. (1994) *J. Biol. Chem. 269*, 4144.

Yu, L., Salzberg, A. A., & Dedon, P. C. (1995) *Bioorg. Med. Chem. 3*, 720−741.

Zegar, I. S., Setayesh, F. R., DeCorte, B. L., Harris, C. M., Harris, T. M., & Stone, M. P. (1996) *Biochemistry 35*, 4334.

BI962957D